

# Reaction Mechanisms of the Proton - Deuteron Breakup Process at GeV Energies

N.B.Ladygina<sup>1</sup>\*, A.V.Shebeko<sup>2</sup>\*\*

<sup>1</sup>Laboratory of High Energies, Joint Institute for Nuclear Research,  
141980 Dubna, Russia,

<sup>2</sup>NSC Kharkov Institute of Physics & Technology, 61108 Kharkov, Ukraine.

**Abstract.** The deuteron fragmentation by fast protons has been studied both near the kinematics of quasi-free proton - proton scattering and far away from it. We have concentrated on the interplay between different reaction mechanisms associated with the antisymmetrization of the initial and final states and rescattering contributions. A multiple-scattering-expansion technique has been applied to evaluate the reaction amplitude. An essential element of this approach in the momentum representation is the use of the effective nucleon-nucleon interaction constructed by Love and Franey as a two-body  $t$ -matrix for the incident proton scattering on a bound nucleon in the deuteron. Along with the five-fold cross sections, the proton analyzing power and the deuteron analyzing powers have been calculated as function of the momentum of the outgoing fast proton. The results are compared with the data obtained by the Gatchina-Saclay collaboration.

## 1 Introduction

Investigations of the proton-deuteron breakup reaction, or more generally of nucleon-deuteron reactions, at high collision energies are usually performed with the aims of studying the internal deuteron structure, of searching for non-nucleonic degrees of freedom, of finding relativistic corrections for the deuteron wave function (DWF), etc. To a great extent, they have been stimulated by relatively simple recipes of the plane-wave impulse approximation (PWIA) for evaluation of the reaction cross sections with unpolarized particles and considering beam and target asymmetries with polarized protons and deuterons. One has to bear in mind that the approximation in its most popular form is equivalent to the so-called spectator reaction mechanism (with the antisymmetrization requirement for three-nucleon states not included). It has already been shown in ref. [1]

\* *E-mail address:* ladygina@sunhe.jinr.ru

\*\* *E-mail address:* shebeko@fbsyst.kharkov.ua

that the spectator approximation, in which one of the nucleons of the deuteron interacts with the incoming proton and the other one remains largely undisturbed, does not describe the inclusive  ${}^1H(d, p)X$  data on the reaction cross section and the tensor asymmetry  $T_{20}$  for the  $0^\circ$ -angle proton emission at deuteron kinetic energies of 1.25 and 2.1 GeV; this is particularly true around the kinematic limit where the dominant reaction channel is  $pd \rightarrow ppn$ . At the same time, according to refs. [2, 3], the inclusion of more complicated reaction mechanisms, such as with the double-scattering (DS) and final-state-interaction (FSI) corrections, to the PWIA results has allowed to improve the theoretical description. A similar trend has been observed when explaining the angular space asymmetry in the deuteron-proton breakup cross sections [4, 5] where one can find an approximate estimation of the respective FSI contributions.

Of course, the understanding of the actual role of two-step reaction mechanisms depends on the reliability of the additional assumptions that are often made within the general approach of formal scattering theory, e.g., the Faddeev scheme for the construction of transition operators between the initial and final three-nucleon states (see the review [6] and refs. therein). In this context, we would like to note that in ref. [3] the author uses just the free nucleon propagator

$$g_0 = [E + i0 - K]^{-1},$$

with  $K$  being the kinetic-energy operator for the three-body system. It enables one to perform the calculations without significant complications, due to the neglect of the principal value part in the decomposition

$$g_0 = P([E - K]^{-1}) - i\pi\delta(E - K),$$

but it has also to be taken with considerable doubt.

In the present work we make another endeavour for a proper description of the exclusive reaction  $pd \rightarrow ppn$  that goes beyond the scope of the PWIA ansatz whose applicability has no firm justification. Therefore, every time, under new kinematic conditions, one has to take care of a coordinated treatment of the structure and rescattering effects (in particular, to separate the reaction mechanism from possible extraordinary deuteron components). Our approach is based on the Faddeev formulation of the multiple-scattering theory for the  $pd$  system and its full breakup. As in ref. [3], we work with the nucleon propagator  $g_0$ . However, unlike ref. [3], we take into account the dependence of the elementary nucleon-nucleon amplitudes on the internal motion of a bound nucleon in the deuteron, which is affected by the interaction with the projectile proton.

Along with the Fermi motion influence some off-shell extrapolations are introduced for these high-energy vertices by using the effective interaction from ref. [7]. Special attention is given to their transformation properties under Lorentz boosts (in particular, the Wigner rotations). In addition, we avoid seemingly artificial truncation in the angular momentum decomposition of high-energy elementary amplitudes, as made in ref. [3].

We apply the matrix inversion method (MIM) [8, 9] when calculating the half-off-energy-shell  $t$ -matrix that determines the rescattering in the final (relatively slow)  $p - n$  pair. The  $p - n$  wave functions in the continuum, constructed within

the MIM, are convenient from an analytical point of view (cf. the studies of the exclusive  $(e, e'p)$  reaction on the deuteron in refs.[10, 11]). Furthermore the spin structure of the elementary amplitudes is fully included. This is of particular significance for the consideration of various polarization observables.

The paper is organized as follows. The underlying formalism and the leading order terms in the  $NN$  t-matrix for obtaining the  $pd \rightarrow ppn$  reaction amplitude are presented in Sec. 2. There one can also find some details concerning the application of the MIM. In Sec. 3 we consider the high-energy  $NN$  vertices and their transformation from the  $NN$  center-of-mass system to the deuteron rest frame (laboratory system). The polarization observables in question are given in Sec.4. The results of our calculations at two kinematics are discussed in Sec.5. We conclude with Sec. 6. Appendix A contains some useful mathematical relations.

## 2 Theoretical Formalism

The differential cross section of the exclusive reaction

$$p(\mathbf{p}) + d(\mathbf{0}) \rightarrow p(\mathbf{p}_1) + p(\mathbf{p}_2) + n(\mathbf{p}_3) \quad (1)$$

for unpolarized particles in the laboratory system can be written as

$$\frac{d^5\sigma}{dp_1 d\Omega_1 d\Omega_2} = \frac{(2\pi)^4}{6} \frac{E_p}{p} \frac{p_1^2 p_2^2 E_2 E_3 |\mathcal{J}|^2}{p_2 E_3 + E_2(p_2 - p \cos\Theta_2 + p_1 \cos\Theta_{12})}, \quad (2)$$

where  $\Theta_2$  is the emission angle for the outgoing slow proton and  $\Theta_{12}$  is the angle between the momenta  $\mathbf{p}_1$  and  $\mathbf{p}_2$  of the fast and the slow protons in the final state (see Fig.1).

We introduce the orthonormal basis

$$\mathbf{z} = \frac{\mathbf{p}}{|\mathbf{p}|}, \quad \mathbf{y} = \frac{\mathbf{p} \times \mathbf{p}_1}{|\mathbf{p} \times \mathbf{p}_1|}, \quad \mathbf{x} = \mathbf{y} \times \mathbf{z} \quad (3)$$

assuming that  $\mathbf{p}$  and  $\mathbf{p}_1$  determine the reaction plane so that  $\mathbf{y}$  is perpendicular to it.

Following the Alt-Grassberger-Sandhas (AGS) formalism of three-body collision theory (see, for instance, refs. [12, 13]), the reaction amplitude  $\mathcal{J}$  is given by the matrix element

$$U_{pd \rightarrow ppn} \equiv \sqrt{2} < 123 | [1 - (1, 2) - (1, 3)] U_{01} | 1(23) > = \delta(\mathbf{p} - \mathbf{p}_1 - \mathbf{p}_2 - \mathbf{p}_3) \mathcal{J} \quad (4)$$

taken on the energy shell:

$$E = E_p + m_d = E_1 + E_2 + E_3. \quad (5)$$

Here  $E$  is the total energy of the three-nucleon system,  $m_d$  the deuteron mass, and  $(i, j)$  the permutation operator for two nucleons. The state  $|1(23) >$  corresponds to the configuration of nucleons 2 and 3 forming the deuteron state and nucleon 1 being the projectile, whereas the state  $< 123 |$  represents the free motion of three nucleons after the reaction and is the product of single nucleon states.

Iterating the AGS equations for the rearrangement operators, one obtains the transition operator  $U_{01}$  as

$$U_{01} = g_0^{-1} + t_2 + t_3 + t_1 g_0 t_2 + t_1 g_0 t_3 + t_2 g_0 t_3 + t_3 g_0 t_2 + O(t^3). \quad (6)$$

By definition,  $t_3 = t_{12}$  is a two-nucleon transition operator (the other can be obtained via cyclic permutations). Obviously, the term  $g_0^{-1}$  does not contribute to the on-shell amplitude (4).

We are interested in such kinematic situations where, firstly, one of the final protons carries away a considerable portion of the initial momentum  $\mathbf{p}$  and, secondly, the momentum  $q = |\mathbf{p} - \mathbf{p}_1|$ , transferred to the p-n pair, is small in comparison with the nucleon mass  $m$ . It enables us to use various nonrelativistic models for the DWF. Under such conditions we retain the first- and second- order contributions to the multiple-scattering expansion (6), neglecting the corrections due to the so-called recoil reaction mechanism for which the high-momentum proton leaves the deuteron without direct knock-out. In addition, small contributions from the DS with participation of a fast nucleon, i.e. the  $t(\text{fast})g_0t(\text{fast})$  terms, are disregarded, what is in accordance with the conclusions in ref. [3]. After this, the matrix element  $U_{pd \rightarrow ppn}$  can be approximated by

$$U_{pd \rightarrow ppn} = \sqrt{2} < 123 | [1 - (2, 3)] [1 + t_{23} g_0] t_{12}^{\text{sym}} | 1(23) > \quad (7)$$

with the symmetrized NN t-operator  $t_{12}^{\text{sym}} = [1 - (1, 2)] t_{12}$ .

The three-body operator  $\omega_{23} \equiv 1 + t_{23} g_0$  acting on the state  $< 123 |$  yields

$$\begin{aligned} < 123 | \omega_{23} &= \lim_{\varepsilon \rightarrow 0+} < 123 | \frac{i\varepsilon}{E + i\varepsilon - K} \left[ 1 + t_{23} \frac{1}{E + i\varepsilon - K} \right] \\ &= \lim_{\varepsilon \rightarrow 0+} < 123 | \frac{i\varepsilon}{E + i\varepsilon - K - V_{23}}, \end{aligned} \quad (8)$$

where  $V_{23}$  is the potential operator of the two-nucleon interaction<sup>1</sup>. Here we have employed the relation

$$\frac{1}{E + i\varepsilon - K - V_{23}} = \frac{1}{E + i\varepsilon - K} + \frac{1}{E + i\varepsilon - K} t_{23} \frac{1}{E + i\varepsilon - K} \quad (9)$$

for the three-body operator  $t_{23}$ , which obeys a Lippmann-Schwinger (LS) equation with  $V_{23}$  as driving term.

Further, since  $K = K_1 + K_2 + K_3$  and, by convention,  $K_i | 123 > = E_i | 123 >$ , one can rewrite Eq. (8) in the form

$$< 123 | \omega_{23} = \lim_{\varepsilon \rightarrow 0+} < 123 | \frac{i\varepsilon}{E - E_1 + i\varepsilon - K_2 - K_3 - V_{23}} \quad (10)$$

or

$$< 123 | \omega_{23} = < 123 | [1 + t_{23}(E - E_1)g_{23}(E - E_1)]. \quad (11)$$

<sup>1</sup>A possible way for the construction of a NN interaction starting from a fundamental Hamiltonian of interacting meson and nucleon fields has been shown recently in ref. [14]

The operator  $g_{23}(E - E_1) \equiv (E - E_1 + i0 - K_2 - K_3)^{-1}$  is a free propagator for the (23)-subsystem, and the scattering operator  $t_{23}(E - E_1)$  satisfies the LS equation

$$t_{23}(E - E_1) = V_{23} + V_{23}g_{23}(E - E_1)t_{23}(E - E_1). \quad (12)$$

Let us rewrite the matrix element (7) indicating explicitly the particle quantum numbers,

$$U_{pd \rightarrow ppn} = \sqrt{2} < \mathbf{p}_1 \mu_1 \tau_1, \mathbf{p}_2 \mu_2 \tau_2, \mathbf{p}_3 \mu_3 \tau_3 | [1 - (2, 3)] \omega_{23} t_{12}^{sym} | \mathbf{p} \mu \tau, \psi_{1M_d 00}(23) >,$$

with the spin and isospin projections denoted as  $\mu$  and  $\tau$  respectively. We assume that  $\tau = \tau_1 = \tau_2 = 1/2$  and  $\tau_3 = -1/2$ . Inserting the unity operator

$$1 = \int d\mathbf{p}' | \mathbf{p}' \mu' \tau' > < \mathbf{p}' \mu' \tau' |,$$

we arrive at the following expression for the reaction amplitude

$$\begin{aligned} \mathcal{J} &= \sum_{TT'} C_{TT'} < \frac{1}{2} \mu_2 \frac{1}{2} \mu_3 | SM_S > < \frac{1}{2} \mu'_2 \frac{1}{2} \mu'_3 | SM'_S > \\ &\int d\mathbf{p}_r' \left\langle \mathbf{p}_r, SM_S \left| 1 + m \frac{t^{ST}(E - E_1)}{\mathbf{p}_r^2 - \mathbf{p}_r'^2 + i0} \right| \mathbf{p}_r', SM'_S \right\rangle \\ &< \mathbf{p}_1 \mu_1, (\mathbf{p}_r' + \mathbf{q}/2) \mu'_2 | t_{sym}^{T'}(E - E'_3) | \mathbf{p} \mu, (\mathbf{p}_r' - \mathbf{q}/2) \mu'' > \quad (13) \\ &< \mu'' \mu'_3 | \psi_{1M_d}(\mathbf{p}_r' - \mathbf{q}/2) > - (2 \leftrightarrow 3), \end{aligned}$$

where  $E'_3 = \sqrt{m_N^2 + (\mathbf{p}_r' - \mathbf{q}/2)^2}$ . Here we have introduced the momentum transfer  $\mathbf{q} = \mathbf{p} - \mathbf{p}_1$ , relative momenta  $\mathbf{p}_r = \frac{1}{2}(\mathbf{p}_2 - \mathbf{p}_3)$  and  $\mathbf{p}_r' = \frac{1}{2}(\mathbf{p}_2' - \mathbf{p}_3')$ , and isotopic coefficients

$$C_{TT'} = \frac{1}{2} \left[ \frac{(-1)^T}{2} \delta_{T'0} + \left( 1 + \frac{(-1)^T}{2} \right) \delta_{T'1} \right]. \quad (14)$$

Henceforth, all summations over dummy discrete indices are implied.

In momentum representation the DWF  $\psi_{1M_d}(\mathbf{k})$  with spin projection  $M_d$  is written as

$$| \psi_{1M_d}(\mathbf{k}) > = \sum_{L=0,2} \sum_{M_L=-L}^L < LM_L 1M_s | 1M_d > u_L(k) Y_L^{M_L}(\hat{k}) | 1M_s >, \quad (15)$$

with the spherical harmonics  $Y_L^{M_L}(\hat{k})$  and the Clebsh-Gordon coefficients in standard form. In our calculations, we have employed the following parametrizations of the S- and D- state wave functions

$$u_0(p) = \sqrt{\frac{2}{\pi}} \sum_i \frac{C_i}{\alpha_i^2 + p^2}, \quad u_2(p) = \sqrt{\frac{2}{\pi}} \sum_i \frac{D_i}{\beta_i^2 + p^2} \quad (16)$$

as proposed in refs. [15, 16].

The wave function of the final p-n pair

$$\begin{aligned} \langle \psi_{\mathbf{p}_r SM_S TM_T}^{(-)} | \mathbf{p}_r' SM_S' TM_T \rangle &= \delta(\mathbf{p}_r - \mathbf{p}_r') \delta_{M_S M_S'} + \\ &\frac{m_N}{\mathbf{p}_r^2 - \mathbf{p}_r'^2 + i0} \langle \mathbf{p}_r SM_S | t^{ST} | \mathbf{p}_r' SM_S' \rangle \end{aligned} \quad (17)$$

contains the FSI part, which can be taken in different ways. First of all, we note that in ref. [4] the t-matrix elements were obtained by solving Eq. (12) with a separable NN interaction. Of course, these solutions are not able to reproduce the off-shell behaviour of the NN t-matrix with more realistic two-body forces. Another approximation relies on the neglect of the principal value part in

$$\frac{1}{\mathbf{p}_r^2 - \mathbf{p}_r'^2 + i0} = -i\pi\delta(\mathbf{p}_r^2 - \mathbf{p}_r'^2) + P \left[ \frac{1}{\mathbf{p}_r^2 - \mathbf{p}_r'^2} \right]. \quad (18)$$

Then, the FSI term can be expressed through the on-energy-shell t-matrix, i.e. the respective phase shifts. Third procedure ( see, ref. [17] and refs. therein) uses some artificial off-shell extrapolation of the t-matrix with energy-dependent prescriptions for the introduction of a proper form factor.

In this paper we use the MIM applied to study the deuteron electrodisintegration [10, 11]. As in ref. [10], we consider the truncated partial-wave expansion,

$$\begin{aligned} \langle \psi_{\mathbf{p}_r SM_S TM_T}^{(-)} | \mathbf{p}_r' SM_S' TM_T \rangle &= \delta_{M_S M_S'} \delta(\mathbf{p}_r - \mathbf{p}_r') + \\ &\sum_{J=0}^{J_{max}} \sum_{M_J=-J}^J Y_l^m(\hat{p}_r) \langle lm SM_S | JM_J \rangle \psi_{ll'}^\alpha(p_r') \langle l' m' SM_S' | JM_J \rangle Y_{l'}^{*m'}(\hat{p}_r'), \end{aligned} \quad (19)$$

where  $J_{max}$  is the maximum value of the total angular momentum in n-p partial waves and  $\alpha = \{J, S, T\}$  is the set of conserved quantum numbers. The radial functions  $\psi_{ll'}^\alpha(p_r')$  are related via

$$\psi_{ll'}^{JST}(p_r') = \sum_{l''} O_{ll''} \varphi_{l''l'}(p_r') - \frac{\delta(p_r' - p_r)}{p_r^2} \delta_{ll'} \quad (20)$$

to the partial wave functions  $\varphi_{l''l'}^\alpha(p_r')$ , which have the asymptotics of standing waves. The coefficients  $O_{ll''}$  can be expressed in terms of the corresponding phase shifts and mixing parameters [10].

Within the MIM, the functions  $\varphi_{ll'}^\alpha(p_r')$  can be represented as

$$\varphi_{ll'}^\alpha(p_r') = \sum_{j=1}^{N+1} B_{ll'}^\alpha(j) \frac{\delta(p_r' - p_j)}{p_j^2}, \quad (21)$$

where the coefficients  $B_{ll'}^\alpha(j)$  fulfill a set of linear algebraic equations approximately equivalent to the  $LS$  integral equation for the  $n - p$  scattering problem. Here  $N$  is the dimension of this set,  $p_j$  are the grid points associated with the Gaussian nodes over the interval  $[-1, 1]$  and  $p_{N+1} = p_0$  (details can be found in ref. [18]). It should be noted that in this way the nucleon wave function is expressed by a series of  $\delta$ -functions allowing one to reduce a triple integral in Eq. (13) to a double one. In addition, the method offers the opportunity to consider the nucleon wave function in the continuum directly in momentum space what simplifies all the calculations a lot.

### 3 High-Energy Vertex and Its Transformations

As seen from Eq. (13), we have to deal with the high-energy matrix elements

$$t^{T'}(E_{on-shell}; \mathbf{p}_1\mu'_1, \mathbf{p}'_2\mu'_2, \mathbf{p}\mu_1, \mathbf{p}'\mu_2) \equiv \langle \mathbf{p}_1\mu'_1, \mathbf{p}'_2\mu'_2 | t^{T'}(E_{on-shell}) | \mathbf{p}\mu_1, \mathbf{p}'\mu_2 \rangle, \quad (22)$$

where  $p_1 \sim p \geq m$  and  $E_{on-shell} \geq 2m$ , which are determined not only on the energy shell

$$E_{\mathbf{p}_1} + E_{\mathbf{p}'_2} = E_{on-shell} = E_{\mathbf{p}} + E_{\mathbf{p}'} \quad (23)$$

but largely beyond it for N-N scattering with arbitrary values of the total momentum  $\mathbf{p} + \mathbf{p}' = \mathbf{p}_1 + \mathbf{p}'_2$  (see Fig. 1). The latter is conserved owing to the requirement of translational invariance.

The frame dependence of these off-shell quantities, in particular, their expression in terms of the  $t$ -matrix elements in the N-N center-of-mass system (c.m.s.) can be found making use of some prescriptions [19, 20] of the relativistic potential theory (RPT) for relating a two-body off-energy-shell  $t$ -matrix between different frames of reference. First, let us recall the equation

$$\begin{aligned} t(E; \mathbf{k}'_1\mu'_1, \mathbf{k}'_2\mu'_2, \mathbf{k}_1\mu_1, \mathbf{k}_2\mu_2) &= N'N \langle \mu'_1 | W^\dagger(\mathbf{u}', \mathbf{k}'_1) | \nu'_1 \rangle \\ &< \mu'_2 | W^\dagger(\mathbf{u}', \mathbf{k}'_2) | \nu'_2 \rangle t(E, \mathbf{K}; \mathbf{k}'^*\nu'_1\nu'_2; \mathbf{k}^*\nu_1, \nu_2) \\ &< \nu_1 | W(\mathbf{u}, \mathbf{k}_1) | \mu_1 \rangle < \nu_2 | W(\mathbf{u}, \mathbf{k}_2) | \mu_2 \rangle, \end{aligned} \quad (24)$$

which connects the on-momentum-shell matrix elements in two bases<sup>2</sup>. One of them,  $\{|\mathbf{k}_1\mu_1, \mathbf{k}_2\mu_2\rangle\}$ , is a direct product  $\{|\mathbf{k}_1\mu_1\rangle \otimes |\mathbf{k}_2\mu_2\rangle\}$  where the single-nucleon states  $|\mathbf{k}_a\mu_a\rangle$  satisfy the following orthonormality and completeness conditions

$$\langle \mathbf{k}'_a\mu'_a | \mathbf{k}_a\mu_a \rangle = \delta(\mathbf{k}'_a - \mathbf{k}_a) \delta_{\mu'_a, \mu_a} \quad (25)$$

and

$$\int d\mathbf{k}_a |\mathbf{k}_a\mu_a\rangle \langle \mathbf{k}_a\mu_a| = 1. \quad (26)$$

By assumption, they are related to the states  $|[m, \frac{1}{2}], \mathbf{k}, \mu\rangle = \sqrt{2E_{\mathbf{k}}} |\mathbf{k}\mu\rangle$  of the so-called canonical basis, which is well known in elementary particle physics (see, e.g., Ch. IV of ref. [21]). The latter is transformed by an irreducible representation of the Lorentz group. In particular, we have under the Lorentz boost  $L(\mathbf{v})$  corresponding to the motion of the reference frame with velocity  $\mathbf{v}$ ,

$$|[m, \frac{1}{2}], \mathbf{k}_a, \mu_a\rangle^{tr} = |[m, \frac{1}{2}], \mathbf{k}_a^{tr}, \nu_a\rangle \langle \nu_a | W(\mathbf{u}, \mathbf{k}_a) | \mu_a \rangle \quad (a = 1, 2), \quad (27)$$

where

$$W(\mathbf{u}, \mathbf{k}_a) = \exp(-i\boldsymbol{\sigma}_a \cdot \boldsymbol{\omega}_a) = \cos \frac{\omega_a}{2} \left\{ 1 - i \frac{\boldsymbol{\sigma}_a \cdot [\mathbf{u} \times \mathbf{k}_a]}{(1 + u_0)m + E_a^{tr} + E_a} \right\} \quad (28)$$

<sup>2</sup>Henceforth, the asterisk is used to mark quantities in the c.m.s.

is the Wigner rotation operator in the spin space of the  $a$ -th nucleon. Here we introduce the four-velocity  $u = (u_0, \mathbf{u}) = (u_0, u_0 \mathbf{v})$  with a Lorentz scalar  $u^2 = 1$  and denote the nucleon energies in the initial and moving frames of reference by  $E_a = \sqrt{\mathbf{k}_a^2 + m^2}$  and  $E_a^{tr} = \sqrt{\mathbf{k}_a^{tr2} + m^2}$ . The angle  $\omega_a$  of this rotation about the axis  $[\mathbf{u} \times \mathbf{k}_a]$  is determined by the relation

$$\tan \frac{\omega_a}{2} = \frac{|[\mathbf{u} \times \mathbf{k}_a]|}{(1 + u_0)m + E_a^{tr} + E_a} \quad (29)$$

(see, for instance, Eq. (32) in ref. [22] or Eq. (C.7) in ref. [11]). In formulae (27)-(29) the symbol  $^{tr}$  belongs to the transformed quantities, so that the transformed four-momentum is

$$k_a^{tr} = (E_a^{tr}, \mathbf{k}_a^{tr}) = L(\mathbf{v})k_a = L(\mathbf{v})(E_a, \mathbf{k}_a). \quad (30)$$

Since we are interested in a specific transition to the N-N c.m.s. simultaneously for the initial and final N-N states, all we need is to put in Eq. (24)  $\mathbf{u} = \mathbf{K}/\sqrt{s}$  and  $\mathbf{u}' = \mathbf{K}'/\sqrt{s'}$ , where  $\mathbf{K} = \mathbf{k}_1 + \mathbf{k}_2 = \mathbf{k}'_1 + \mathbf{k}'_2 = \mathbf{K}'$  is the total momentum of the initial(final) N-N pair. Normally, the Lorentz scalars  $s$  and  $s'$  are defined as  $s = (k_1 + k_2)^2 = E^{*2}$  and  $s' = (k'_1 + k'_2)^2 = E'^{*2}$ .

The corresponding basis  $\{|\mathbf{K}\mathbf{k}^* \mu_1 \mu_2\rangle\}$  is composed of two-nucleon states with relative momentum  $\mathbf{k}^*$  between two nucleons, measured in their c.m.s., and total momentum  $\mathbf{K}$ . In accordance with the customary recipes (see, for instance, Sect. 28 in ref. [23]), every state  $|\mathbf{K}\mathbf{k}^* \mu_1 \mu_2\rangle$  can be represented as a product state  $|[m, \frac{1}{2}], \mathbf{k}^*, \mu_1\rangle | [m, \frac{1}{2}], -\mathbf{k}^*, \mu_2\rangle$  which is subject to a subsequent Lorentz boost with velocity  $\mathbf{u} = -\mathbf{K}/E^*$ . Doing so, we get

$$|\mathbf{K}\mathbf{k}^* \mu_1 \mu_2\rangle = N |\mathbf{k}_1 \nu_1\rangle |\mathbf{k}_2 \nu_2\rangle \langle \nu_1 | W^\dagger(\mathbf{K}/E^*, \mathbf{k}_1) | \mu_1 \rangle \langle \nu_2 | W^\dagger(\mathbf{K}/E^*, \mathbf{k}_2) | \mu_2 \rangle. \quad (31)$$

We have used the property  $W(-\mathbf{u}, \mathbf{k}) = W^\dagger(\mathbf{u}, \mathbf{k})$  and the relations  $W(\mathbf{K}/E^*, \mathbf{k}^*) = W(\mathbf{K}/E^*, \mathbf{k}_1)$  and  $W(\mathbf{K}/E^*, -\mathbf{k}^*) = W(\mathbf{K}/E^*, \mathbf{k}_2)$ . In this context, note that for given momenta  $\mathbf{k}_1$  and  $\mathbf{k}_2$  in an arbitrary frame of reference

$$\mathbf{k}^* = \mathbf{k}_1^* = -\mathbf{k}_2^* = \frac{E_2 + E_2^*}{E_1 + E_2 + E^*} \mathbf{k}_1 - \frac{E_1 + E_1^*}{E_1 + E_2 + E^*} \mathbf{k}_2, \quad (32)$$

where  $E^* = E_1^* + E_2^*$  is the respective invariant mass (the total energy in the c.m.s.).

In order to provide the orthonormality and completeness relations

$$\langle \mathbf{K}' \mathbf{k}'^* \mu'_1 \mu'_2 | \mathbf{K} \mathbf{k}^* \mu_1 \mu_2 \rangle = \delta(\mathbf{K}' - \mathbf{K}) \delta(\mathbf{k}'^* - \mathbf{k}^*) \delta_{\mu'_1, \mu_1} \delta_{\mu'_2, \mu_2} \quad (33)$$

and

$$\int d\mathbf{K} d\mathbf{k}^* |\mathbf{K} \mathbf{k}^* \mu_1 \mu_2\rangle \langle \mathbf{K} \mathbf{k}^* \mu_1 \mu_2| = 1 \quad (34)$$

the normalization factor  $N$  in Eq. (31) (see also Eq. (24)) should be

$$N = [J(\mathbf{k}_1, \mathbf{k}_2)]^{-\frac{1}{2}}, \quad (35)$$



where  $J(\mathbf{k}_1, \mathbf{k}_2)$  is the Jacobian for the transformation between the  $\mathbf{k}_1 \mathbf{k}_2$  – and  $\mathbf{K} \mathbf{k}^*$  – representations, i.e.

$$J(\mathbf{k}_1, \mathbf{k}_2) = \frac{E_1^* + E_2^*}{E_1 + E_2} \frac{E_1 E_2}{E_1^* E_2^*}. \quad (36)$$

Analogously, one has

$$J(\mathbf{k}'_1, \mathbf{k}'_2) = \frac{E_1'^* + E_2'^*}{E_1' + E_2'} \frac{E_1' E_2'}{E_1'^* E_2'^*}, \quad (37)$$

and the normalization factor  $N'$  for the final N-N pair is

$$N' = [J(\mathbf{k}'_1, \mathbf{k}'_2)]^{-\frac{1}{2}}. \quad (38)$$

The next result [20]

$$t(E; \mathbf{K}; \mathbf{k}^* \nu'_1 \nu'_2; \mathbf{k}^* \nu_1, \nu_2) = Ft(\sqrt{E^2 - \mathbf{K}^2}; \mathbf{k}^* \nu'_1 \nu'_2; \mathbf{k}^* \nu_1, \nu_2), \quad (39)$$

with

$$F = \frac{E}{\sqrt{E^2 - \mathbf{K}^2}} \frac{\sqrt{E^2 - \mathbf{K}^2} + \sqrt{(E'_1 + E'_2)^2 - \mathbf{K}^2}}{E + E'_1 + E'_2} \frac{\sqrt{E^2 - \mathbf{K}^2} + \sqrt{(E_1 + E_2)^2 - \mathbf{K}^2}}{E + E_1 + E_2}, \quad (40)$$

enables one to express the fully-off-shell matrix elements with nonzero total momentum through the others with zero total momentum. The latter are the fully-off-shell  $t$ -matrix elements in the c.m.s..

Using Eqs. (24) and (39) in our evaluation of the matrix elements (22), we approximate them with the ones in the N-N laboratory system (LAB) with  $\mathbf{p}' = 0$ . This appears to be reasonable since  $\mathbf{p}' = \mathbf{p}'_r - \mathbf{q}/2$  (see Eq. (13)) is an internal nucleon momentum in the deuteron. In addition, we neglect the deuteron binding energy, and thus

$$E_{on-shell} = E_{\mathbf{p}} + m \equiv E, \quad E' = E'_1 + E'_2 = E_{\mathbf{p}_1} + E_{\mathbf{p}_2}, \\ s = 2mE, \quad s' = E'^2 - \mathbf{p}^2.$$

Of course, in order to avoid any confusion, one should distinguish between the total two-body energy  $E$  in this section and the collision energy in Eq. (5).

Then the transformation of interest for this half-off-shell  $t$ -matrix can be written in the compact form,

$$t^{LAB} \equiv t^{T'}(E; \mathbf{p}_1 \mu'_1, \mathbf{q} \mu'_2, \mathbf{p} \mu_1, \mathbf{0} \mu_2) = \Phi W^\dagger(\mathbf{u}', \mathbf{p}_1) W^\dagger(\mathbf{u}', \mathbf{q}) t^{CM} \quad (41)$$

with

$$\Phi = \frac{1}{4} \sqrt{\frac{ss'}{mE_{\mathbf{p}'_2} E_{\mathbf{p}} E_{\mathbf{p}_1}}} \sqrt{\frac{EE'}{\sqrt{ss'}}} \frac{\sqrt{s} + \sqrt{s'}}{E + E'} \quad (42)$$

or

$$\Phi = \sqrt{\left(1 - \frac{T_{\mathbf{p}}}{2E_{\mathbf{p}}}\right) \left(1 - \frac{T_{\mathbf{p}_1}}{2E_{\mathbf{p}_1}}\right)} \sqrt{\frac{EE'}{4mE_{\mathbf{p}'_2}} \frac{\sqrt{s} + \sqrt{s'}}{E + E'}}, \quad (43)$$

where  $T_{\mathbf{p}}$  ( $T_{\mathbf{p}_1}$ ) is the kinetic energy of the incident (outgoing) proton, and  $t^{CM} \equiv t(\sqrt{s}; \mathbf{k}^{*'}; \mathbf{k}^*)$  is the half-off-shell  $t$ -matrix in the N-N c.m.s. Further, a simple calculation yields

$$W^\dagger(\mathbf{u}', \mathbf{p}_1) = \cos \frac{\omega_1}{2} [1 + i\boldsymbol{\sigma}_1 \cdot \mathbf{y} \tan \frac{\omega_1}{2}], \quad (44)$$

and

$$W^\dagger(\mathbf{u}', \mathbf{q}) = \cos \frac{\omega_2}{2} [1 - i\boldsymbol{\sigma}_2 \cdot \mathbf{y} \tan \frac{\omega_2}{2}], \quad (45)$$

with

$$\tan \frac{\omega_1}{2} = \frac{p}{\sqrt{s'}} \frac{p_1}{K_1} \sin \theta_1, \quad (46)$$

and

$$\tan \frac{\omega_2}{2} = \frac{p}{\sqrt{s'}} \frac{p_1}{K_2} \sin \theta_1, \quad (47)$$

where  $\theta_1$  is the angle between the momenta  $\mathbf{p}$  and  $\mathbf{p}_1$ , i.e. the emission angle of the fast proton in the deuteron rest frame. Explicit expressions for the coefficients  $K_1$  and  $K_2$  are given in the Appendix. From Eqs. (44) and (45) we see that the Wigner operators correspond to rotations in opposite directions about the  $\mathbf{y}$ -axis normal to the reaction plane.

When evaluating the half-off-shell elements  $t(\sqrt{s}; \mathbf{k}^{*'}; \mathbf{k}^*)$  in Eq. (41) we have started with the Love-Franey model used to construct the on-shell N-N  $t$ -matrix in each N-N channel (triplet-odd, triplet-even, etc.). According to ref. [7] (see Eq. (12) in the first paper), the corresponding matrix elements are expressed through the effective N-N interaction operators sandwiched between the initial and final plane-wave states. We extend this construction to the off-shell case using the same operators with complex strengths depending on  $\sqrt{s}$  and allowing the initial and final momenta to assume the current values of  $\mathbf{k}^*$  and  $\mathbf{k}^{*'}$ . Obviously, such an off-shell extrapolation does not change the general spin structure

$$\begin{aligned} t_{NN}^{CM} = & A + B(\boldsymbol{\sigma}_1 \hat{n}^*)(\boldsymbol{\sigma}_2 \hat{n}^*) + C(\boldsymbol{\sigma}_1 + \boldsymbol{\sigma}_2) \cdot \hat{n}^* + \\ & D(\boldsymbol{\sigma}_1 \hat{q}^*)(\boldsymbol{\sigma}_2 \hat{q}^*) + F(\boldsymbol{\sigma}_1 \hat{Q}^*)(\boldsymbol{\sigma}_2 \hat{Q}^*), \end{aligned}$$

where

$$\hat{q}^* = \frac{\mathbf{k}^* - \mathbf{k}^{*'}}{|\mathbf{k}^* - \mathbf{k}^{*'}|}, \quad \hat{Q}^* = \frac{\mathbf{k}^* + \mathbf{k}^{*'}}{|\mathbf{k}^* + \mathbf{k}^{*'}|}, \quad \hat{n}^* = \frac{\mathbf{k}^* \times \mathbf{k}^{*'}}{|\mathbf{k}^* \times \mathbf{k}^{*'}|}, \quad (48)$$

inherent in the on-shell N-N  $t$ -matrix in c.m.s. (see, for instance, ref. [24]). Of course, this structure is subject to certain changes under the transformation (41) so that

$$\begin{aligned} t_{NN}^{lab} = & \cos \frac{\omega_1}{2} \cos \frac{\omega_2}{2} \Phi \{ F_1 + F_2(\boldsymbol{\sigma}_1 \mathbf{y}) + F_3(\boldsymbol{\sigma}_2 \mathbf{y}) + F_4(\boldsymbol{\sigma}_1 \mathbf{x})(\boldsymbol{\sigma}_2 \mathbf{x}) + \\ & F_5(\boldsymbol{\sigma}_1 \mathbf{y})(\boldsymbol{\sigma}_2 \mathbf{y}) + F_6(\boldsymbol{\sigma}_1 \mathbf{z})(\boldsymbol{\sigma}_2 \mathbf{z}) + F_7(\boldsymbol{\sigma}_1 \mathbf{x})(\boldsymbol{\sigma}_2 \mathbf{z}) + F_8(\boldsymbol{\sigma}_1 \mathbf{z})(\boldsymbol{\sigma}_2 \mathbf{x}) \}. \end{aligned} \quad (49)$$

Relationships between the structure functions  $F_i$  in the laboratory and  $A$  to  $F$  in the center- of -mass systems are given in the Appendix.

#### 4 Polarization Observables for Proton-Deuteron Breakup.

The reaction amplitude  $\mathcal{J}$  resulting from our calculation, allows us to find the spin polarization coefficients

$$C_{i,j,k,l,n} = \frac{1}{C_0} \text{Tr} \left\{ \mathcal{J} \mathcal{P}_i \sigma_j \mathcal{J}^\dagger \sigma_k \sigma_l \sigma_n \right\} \quad (50)$$

with

$$C_0 = \text{Tr} \left\{ \mathcal{J} \mathcal{J}^\dagger \right\}, \quad (51)$$

where the first and second indices  $i$  and  $j$  refer to the deuteron and the incident proton polarizations, respectively, and the remaining ones specify the nucleon polarizations in the final state. The standard operators  $\mathcal{P}_i (i = 0, 1, \dots, 9)$  introduced by Goldfarb (see, e.g., Eqs. (2.17) in ref. [25]) form the basis for the  $3 \times 3$  spin 1 space. If a particle in the entrance channel is unpolarized or the polarization of a final nucleon is not analyzed, the corresponding index is assumed equal to zero.

In this paper, we consider the first-order observables related to the polarization of initial particles for coplanar geometry. In this context, let us determine the analyzing power of the projectile proton

$$C_{0,y,0,0,0} = \frac{2}{C_0} \text{Im} \sum \langle m_1, m_2, m_3 | \mathcal{J} | \frac{1}{2} M_d \rangle \langle M_d, -\frac{1}{2} | \mathcal{J} | m_1, m_2, m_3 \rangle^*, \quad (52)$$

and the vector and tensor analyzing powers of the deuteron

$$\begin{aligned} C_{y,0,0,0,0} &= \frac{\sqrt{2}}{C_0} \text{Im} \sum \{ \langle m_1, m_2, m_3 | \mathcal{J} | m1 \rangle \langle 0m | \mathcal{J} | m_1, m_2, m_3 \rangle^* - \\ &\quad \langle m_1, m_2, m_3 | \mathcal{J} | m-1 \rangle \langle 0m | \mathcal{J} | m_1, m_2, m_3 \rangle^* \}, \\ C_{yy,0,0,0,0} &= -\frac{1}{2C_0} \sum \{ | \langle m_1, m_2, m_3 | \mathcal{J} | m1 \rangle |^2 + | \langle m_1, m_2, m_3 | \mathcal{J} | m-1 \rangle |^2 - \\ &\quad 2 | \langle m_1, m_2, m_3 | \mathcal{J} | m0 \rangle |^2 + \\ &\quad 6 \text{Re} \langle m_1, m_2, m_3 | \mathcal{J} | m1 \rangle \langle -1m | \mathcal{J} | m_1, m_2, m_3 \rangle^* \} \\ C_{zz,0,0,0,0} &= \frac{1}{C_0} \sum \{ | \langle m_1, m_2, m_3 | \mathcal{J} | m1 \rangle |^2 + | \langle m_1, m_2, m_3 | \mathcal{J} | m-1 \rangle |^2 - \\ &\quad 2 | \langle m_1, m_2, m_3 | \mathcal{J} | m0 \rangle |^2 \}. \end{aligned} \quad (53)$$

Of course, the symbol  $\sum$  means summation over the particle spin projections. Here, unlike in Eq. (13) (more exactly, in its l.h.s.), these projections are explicitly indicated. As a consequence of parity conservation, the vector analyzing powers of the deuteron  $C_{x,0,0,0,0}$ ,  $C_{z,0,0,0,0}$  and the proton  $C_{0,x,0,0,0}$ ,  $C_{0,z,0,0,0}$  are equal to zero in coplanar geometry. Moreover, the tensor analyzing power  $C_{xx,0,0,0,0}$  is not independent owing to the relation  $C_{xx,0,0,0,0} + C_{yy,0,0,0,0} + C_{zz,0,0,0,0} = 0$  (cf. Eq. (2.18) of ref. [25]). Thus, we have only the above four independent first-order observables.

## 5 Results and Discussion

Using expression (13) for the reaction amplitude, the exclusive cross sections and the first-order polarization observables have been calculated at a projectile energy of 1 GeV in the deuteron rest frame. All the calculations have been performed with the Paris potential [15]. We have confined ourselves to the coplanar geometry (with momentum  $\mathbf{p}_2$  lying in the reaction plane) and considered two kinematics.

Kinematics I is equivalent to the Gatchina experiment [17, 26] as the  $pp$  coincidence cross sections have been measured on the left of the quasi-free peak (QFP), far from its maximum (Fig. 2). Recall that the latter corresponds to proton elastic scattering on a free proton at rest in case of a spectator momentum  $p_3 = 0$ . In fact, the four-momentum conservation for reaction (1) in the deuteron rest frame yields the Bjorken variable  $x = q_\mu^2/(2m\omega) = 1$ , where  $q_\mu^2 = \mathbf{q}^2 - \omega^2 = -t$ . Of course, the equality  $x = 1$  is valid only up to small corrections due to binding effects in the deuteron. The FSI distortions have been taken into account in  $p - n$  partial scattering states with  $J_{max}=2,3$ , and 4. We see that the results obtained for the case with  $J_{max} = 3$  are practically converged and may be assigned a reasonable predictive power (cf. Figs. 2-6).

The experimental conditions have been chosen so that FSI contributions could be neglected. Indeed, the FSI give insignificant corrections for the differential cross section with respect to the PWIA predictions (Fig. 2). However, their effects are more pronounced for the polarization observables. In this connection, especially the tensor analyzing power of the deuteron  $C_{yy,0,0,0,0}$  (Fig. 5) and the vector analyzing power of the proton  $C_{0,y,0,0,0}$  (Fig. 3) are of great interest. Note in particular that the PWIA curve for  $C_{yy,0,0,0,0}$  (Fig. 5) has a very quickly changing behaviour and comes from a negative region up to nearly the upper limit of 1 while the full result lies only in the positive region, has a modest slope and varies from  $\sim 0.5$  to  $0.8$ . We observe a different behaviour for the other tensor analyzing power of the deuteron  $C_{zz,0,0,0,0}$  (Fig. 6). One can see that this observable in PWIA assumes small negative values while the calculations taking account of the FSI produce a positive result with very quickly changing values. In addition, the result obtained with  $J_{max} = 2$  is significantly different from the one with  $J_{max} = 3$ , what is not so evident for the other observables. For the vector analyzing powers of the proton  $C_{0,y,0,0,0}$  (Fig. 3) and the deuteron  $C_{y,0,0,0,0}$  (Fig. 4) the PWIA and FSI curves have a similar behaviour, but their absolute values are about two to three times different. Thus, we can conclude that the polarization observables are very sensitive to reaction mechanisms. Unfortunately, only the differential cross section has been measured under such kinematic conditions.

The same observables in kinematics II are presented in Figs. 7-11. The projectile proton energy is 1 GeV as in the previous case. The scattering angles of the fast and slow protons are  $\theta_1 = 6.77^\circ$  and  $\theta_2 = 83^\circ$ , respectively. In such kinematics we have more favourable conditions for the applicability of our approach. Really, while the  $q$  ( $p_3$ ) - values for kinematics I range from 500 (300) to 650 (570) MeV/c, the momentum transfer  $q$  and the neutron momentum  $p_3$  for the kinematics II with a cut at  $p_1 = 1.60$  GeV/c do not exceed, respectively,  $q_{max} = 217$  MeV/c and  $p_3^{max} = 180$  MeV/c which is in complete accordance with

the underlying assumptions.

The FSI corrections calculated for  $J_{max}=1$  and 2, are denoted by the dash-dotted and solid lines, respectively. The agreement between them is quite satisfactory, especially for the differential cross section (Fig. 7), where the lines for  $J_{max}=1$  and 2 are indistinguishable. As before, the PWIA predictions are denoted by dashed lines in all the figures (Figs.7-11).

Unlike the picture in Fig. 2, the  $p_1$ -dependence of the reaction cross section displayed for kinematics II in Fig. 7 covers the QFP region up to its boundary, i.e., the maximum  $p_1$  value is allowed under the condition  $p_r = 0$ . There has been the expectation that the FSI influence is negligible in the QFS region. However, as is evident from Fig. 7, the differential cross section is  $\sim 2$  times smaller relative to the PWIA predictions in the QFS region due to the FSI effects. It is the consequence of the vicinity of the two peaks (QFS and FSI). It is interesting to note that the PWIA and FSI predictions for the polarization observables (Figs.8-11) in the QFS region practically coincide while these observables change their behaviors very quickly when going to the FSI region.

## 6 Conclusion

In the present paper we have explored a reasonable approximation to treat the deuteron-proton breakup reaction in the GeV-region. The employed approach incorporates the leading terms in the multiple scattering expansion of the reaction transition operator in the  $N - N$  t-matrix. Our consideration is free from shortcomings made in earlier theoretical studies of this process. The differential cross sections and the first-order polarization observables have been calculated under the two kinematic conditions (one of them corresponding to the Gatchina experiment). These calculations have shown that the FSI contributions are very important to describe deuteron breakup by the proton in the GeV-region. We have seen that the FSI effects, dependent on kinematic conditions, appear in different ways. They can slightly change the corresponding cross section with unpolarized observables and vice versa. Therefore, studying the deuteron structure (especially, the non-nucleonic degrees of freedom in the deuteron) by high-energy breakup reactions, one should make every effort to include FSI corrections.

*Acknowledgement.* The authors are thankful to V.P. Ladygin for helpful discussions and permanent interest in this work. They thank also O.G.Grebenyuk for information about experimental data. A.S. is very grateful to V.V. Glagolev for support and hospitality during his visits to the LHE of the JINR,Dubna.

## Appendix

The NN amplitudes  $F_i$  in the laboratory frame are related to A-F, the ones in the center-of-mass system by

$$\begin{aligned} F_1 &= A + B \frac{U^2}{K_1 K_2} + iCU \left( \frac{1}{K_1} - \frac{1}{K_2} \right) \\ F_2 &= iU \left( \frac{A}{K_1} - \frac{B}{K_2} \right) + C \left( 1 + \frac{U^2}{K_1 K_2} \right) \end{aligned}$$

$$\begin{aligned}
F_3 &= -iU \left( \frac{A}{K_2} - \frac{B}{K_1} \right) + C \left( 1 + \frac{U^2}{K_1 K_2} \right) \\
F_4 &= D \left\{ (\hat{q}^* \mathbf{x}) - \frac{U}{K_1} (\hat{q}^* \mathbf{z}) \right\} \left\{ (\hat{q}^* \mathbf{x}) + \frac{U}{K_2} (\hat{q}^* \mathbf{z}) \right\} + F \left\{ (\hat{Q}^* \mathbf{x}) - \frac{U}{K_1} (\hat{Q}^* \mathbf{z}) \right\} \left\{ (\hat{Q}^* \mathbf{x}) + \frac{U}{K_2} (\hat{Q}^* \mathbf{z}) \right\} \\
F_5 &= A \frac{U^2}{K_1 K_2} + B + iCU \left( \frac{1}{K_1} - \frac{1}{K_2} \right) \\
F_6 &= D \left\{ (\hat{q}^* \mathbf{z}) + \frac{U}{K_1} (\hat{q}^* \mathbf{x}) \right\} \left\{ (\hat{q}^* \mathbf{z}) - \frac{U}{K_2} (\hat{q}^* \mathbf{x}) \right\} + F \left\{ (\hat{Q}^* \mathbf{z}) + \frac{U}{K_1} (\hat{Q}^* \mathbf{x}) \right\} \left\{ (\hat{Q}^* \mathbf{z}) - \frac{U}{K_2} (\hat{Q}^* \mathbf{x}) \right\} \\
F_7 &= D \left\{ (\hat{q}^* \mathbf{x}) - \frac{U}{K_1} (\hat{q}^* \mathbf{z}) \right\} \left\{ (\hat{q}^* \mathbf{z}) - \frac{U}{K_2} (\hat{q}^* \mathbf{x}) \right\} + F \left\{ (\hat{Q}^* \mathbf{x}) - \frac{U}{K_1} (\hat{Q}^* \mathbf{z}) \right\} \left\{ (\hat{Q}^* \mathbf{z}) - \frac{U}{K_2} (\hat{Q}^* \mathbf{x}) \right\} \\
F_8 &= D \left\{ (\hat{q}^* \mathbf{z}) + \frac{U}{K_1} (\hat{q}^* \mathbf{x}) \right\} \left\{ (\hat{q}^* \mathbf{x}) + \frac{U}{K_2} (\hat{q}^* \mathbf{z}) \right\} + F \left\{ (\hat{Q}^* \mathbf{z}) + \frac{U}{K_1} (\hat{Q}^* \mathbf{x}) \right\} \left\{ (\hat{Q}^* \mathbf{x}) - \frac{U}{K_2} (\hat{Q}^* \mathbf{z}) \right\}.
\end{aligned}$$

Here we have introduced

$$\begin{aligned}
U &= \frac{|\mathbf{p} \times \mathbf{p}_1|}{\sqrt{s'}} = \frac{pp_1 \sin \theta_1}{\sqrt{s'}} \\
s &= (p + p')^2, \quad s' = (p_1 + p_2')^2 \\
u_0 &= \frac{E_p + m}{\sqrt{s}} \quad u'_0 = \frac{E_{p_1} + E_{p_2'}}{\sqrt{s'}}
\end{aligned}$$

$$\begin{aligned}
K_1 &= \frac{1}{2}(u'_0 + 1)(2m + \sqrt{s'}) + \frac{1}{2}(E_{p_1} - E_{p_2'}) \\
K_2 &= \frac{1}{2}(u'_0 + 1)(2m + \sqrt{s'}) - \frac{1}{2}(E_{p_1} - E_{p_2'}).
\end{aligned}$$

The vectors  $\mathbf{q}^*$  and  $\mathbf{Q}^*$  defined in the c.m.s. can be written in the lab. system as

$$\begin{aligned}
(\mathbf{q}^* \mathbf{x}) &= -(\mathbf{Q}^* \mathbf{x}) = -p_1 \sin \theta_1 \\
(\mathbf{q}^* \mathbf{z}) &= -p_1 \cos \theta_1 + p \left\{ \frac{m + \sqrt{s}/2}{\sqrt{s}(1 + u_0)} + \frac{E_{p_1} + \sqrt{s'}/2}{\sqrt{s'}(1 + u'_0)} \right\} \\
(\mathbf{Q}^* \mathbf{z}) &= p_1 \cos \theta_1 + p \left\{ \frac{m + \sqrt{s}/2}{\sqrt{s}(1 + u_0)} - \frac{E_{p_1} + \sqrt{s'}/2}{\sqrt{s'}(1 + u'_0)} \right\},
\end{aligned}$$

and their moduli are expressed through the invariants  $s$  and  $t$  via

$$\mathbf{q}^{*2} = \frac{1}{4}(\sqrt{s} - \sqrt{s'})^2 - t, \quad \mathbf{Q}^{*2} = \frac{1}{4}(\sqrt{s} + \sqrt{s'})^2 + t - 4m^2.$$

## References

- Perdrisat, C.F., Punjabi, V., Lyndon, C., Yonnet, J., Beurtey, R., Boivin, M., Boudard, A., Plouin, F., Didelez, J.P., Frascaria, R., Reposeur, T., Siebert, R., Warde, E., Gugelot, P.C., Grossiord, J.Y.: Phys. Rev.Lett. **59**, 2840 (1987);  
Punjabi, V., Perdrisat, C.F., Ulmer, P., Lyndon, C., Yonnet, J., Beurtey, R., Boivin, M., Plouin, F., Boudard, A., Didelez, J.P., Frascaria, R., Reposeur, T., Siebert, R., Warde, E., Gugelot, P.C.: Phys. Rev. **C39**, 608 (1989)
- Perdrisat, C. F., Punjabi, V.: Phys. Rev. **C42**, 1899 (1990)
- Zborovsky, I.: Z. Phys. **A343**, 347 (1992)
- Aladashvili, B. S., Germond, G.-F., Glagolev, V. V., Nioradze, M. S., Siemiarczuk, T., Stepaniak, J., Streltsov, V.N., Wilkin, C., Zielinski, P.: J. Phys. G: Nucl. Phys. **3**, 7 (1977)
- Glagolev, V. V., Hlavacova, J., Kacharava, A.K., Khairtdinov, K.U., Ladygina, N.B., Lebedev, R.M., Mamulashvili, A.G., Martinska, G., Nioradze, M.S., Pastircak, B., Pestova, G.D., Sandor, L., Shimansky, S.S., Siemiarczuk, T., Stepaniak, J., Urban, J.: Phys. Atom. Nucl. **59**, 2125 (1996)

6. Glöckle, W., Witala, H., Hüber, D., Kamada, H., Golak, J.: Phys. Rep. **274**, 109 (1996)
7. Love, W. G., Franey, M. A.: Phys. Rev. **C24**, 1073 (1981); Love, W.G., Franey, M.A.: *ibid.* **C31**, 488 (1985)
8. Haftel, M.I., Tabakin, F.: Nucl. Phys. **A158**, 1 (1970)
9. Brown, G. E., Jackson, A. D., Kuo, T. T. S.: Nucl. Phys. **A133**, 481 (1969)
10. Korchin, A. Yu., Mel'nik, Yu. P., Shebeko, A. V.: Few-Body Syst. **9**, 211 (1990)
11. Mel'nik, Yu. P., Shebeko, A.V.: Few-Body Syst. **13**, 59 (1992)
12. Schmid, E., Ziegelmann, H.: The Quantum Mechanical Three-Body Problem. Oxford: Pergamon Press 1974
13. Glöckle, W.: The Quantum Mechanical Few-Body Problem. Berlin: Springer Verlag 1983
14. Shebeko, A. V., Shirokov, M. I.: Prog. Part. Nucl. Phys. **44**, 75 (2000)
15. Lacombe, M., Loiseau, B., Richard, J. M., Vinh Mau, R., Cote, J., Pires, P., de Tourreil, R.: Phys. Rev. **C21**, 861 (1980)
16. Machleidt, R., Holinde, K., Elster, C.: Phys. Rep. **149**, 1 (1987).
17. Aleshin, N. P., Belostotski, S. L., Grebenyuk, O. G., Gordeev, V. A., Komarov, E. N., Kochenda, L. M., Lasarev, V. I., Manayenkov, S. I., Miklukho, O. V., Nelyubin, V. V., Nikulin, V. N., Prokofiev, O. E., Sulimov, V. V., Vikhrov, V. V., Boudard, A., Laget, J.-M.: Nucl. Phys. **A568**, 809 (1994)
18. Korchin, A. Yu., Shebeko, A.V.: Preprint KFTI 77-35, Kharkov 1977
19. Heller, L., Bohannon, G. E., Tabakin, F.: Phys. Rev. **C13**, 742 (1976)
20. Garcilazo, H.: Phys. Rev. **C16**, 1996 (1976)
21. Gasiorowicz, S.: Elementary Particle Physics. New York: Wiley 1966
22. Ritus, V. I.: JETP **40**, 352 (1961)
23. Werle, J.: Relativistic Theory of Reactions. Warszawa: Polish Sci. Publ. 1966
24. Goldberger, M., Watson, K.: Collision Theory. New York: Wiley 1964
25. Ohlsen, G. O.: Rep. Prog. Phys. **35**, 717 (1972)
26. Grebenyuk, O.G.: Private communication. The data in Table 7 of ref. [17] should be scaled by a factor of 10.

## Figures.

**Fig.1** Kinematic variables for the  $pd \rightarrow ppn$  reaction in the deuteron rest frame.

**Fig.2** The breakup differential cross section at  $\theta_1 = 15^\circ$ ,  $\theta_2 = 78^\circ$  [17] plotted versus the fast proton momentum  $p_1$  in the deuteron rest frame. The dashed line corresponds to the PWIA; the dotted, dash-dotted and solid curves represent the full calculation with  $J_{max} = 2, 3$ , and 4, respectively.

**Fig.3** The  $p_1$ -dependence of the vector analyzing power of the initial proton  $C_{0,y,0,0,0}$  at  $\theta_1 = 15^\circ$ ,  $\theta_2 = 78^\circ$ . Notations as in Fig.2.

**Fig.4** The  $p_1$ -dependence of the deuteron vector analyzing power  $C_{y,0,0,0,0}$  at  $\theta_1 = 15^\circ$ ,  $\theta_2 = 78^\circ$ . Notations as in Fig.2.

**Fig.5** The  $p_1$ -dependence of the deuteron tensor analyzing power  $C_{yy,0,0,0,0}$  at  $\theta_1 = 15^\circ$ ,  $\theta_2 = 78^\circ$ . Notations as in Fig.2.

**Fig.6** The  $p_1$ -dependence of the deuteron tensor analyzing power  $C_{zz,0,0,0,0}$  at  $\theta_1 = 15^\circ$ ,  $\theta_2 = 78^\circ$ . Notations as in Fig.2.

**Fig.7** The breakup differential cross section at  $\theta_1 = 6.77^\circ$ ,  $\theta_2 = 83^\circ$  plotted versus the fast proton momentum  $p_1$  in the deuteron rest frame. The dashed line corresponds to the PWIA; the dash-dotted and solid curves represent the full calculation with  $J_{max} = 1$  and 2, respectively.

**Fig.8** The same as in Fig. 3 at  $\theta_1 = 6.77^\circ$ ,  $\theta_2 = 83^\circ$ . Notations as in Fig. 7.

**Fig.9** The same as in Fig. 4 at  $\theta_1 = 6.77^\circ$ ,  $\theta_2 = 83^\circ$ . Notations as in Fig. 7.

**Fig.10** The same as in Fig. 5 at  $\theta_1 = 6.77^\circ$ ,  $\theta_2 = 83^\circ$ . Notations as in Fig. 7.

**Fig.11** The same as in Fig. 6 at  $\theta_1 = 6.77^\circ$ ,  $\theta_2 = 83^\circ$ . Notations as in Fig. 7.



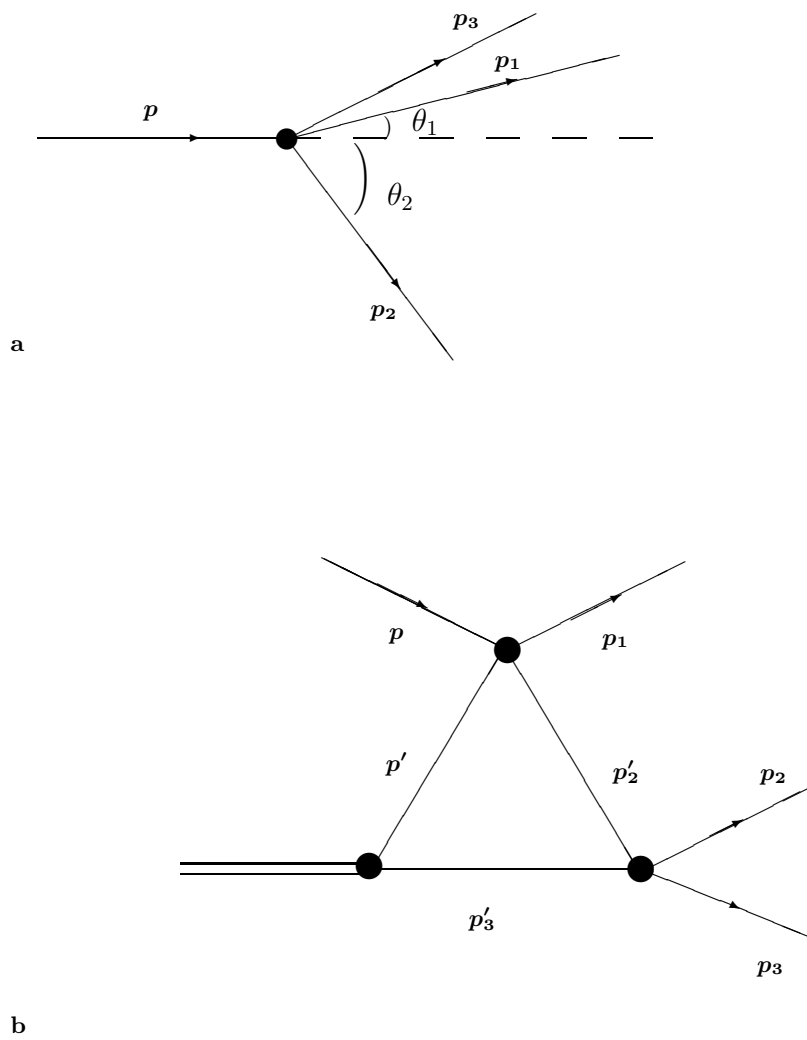


Fig.1

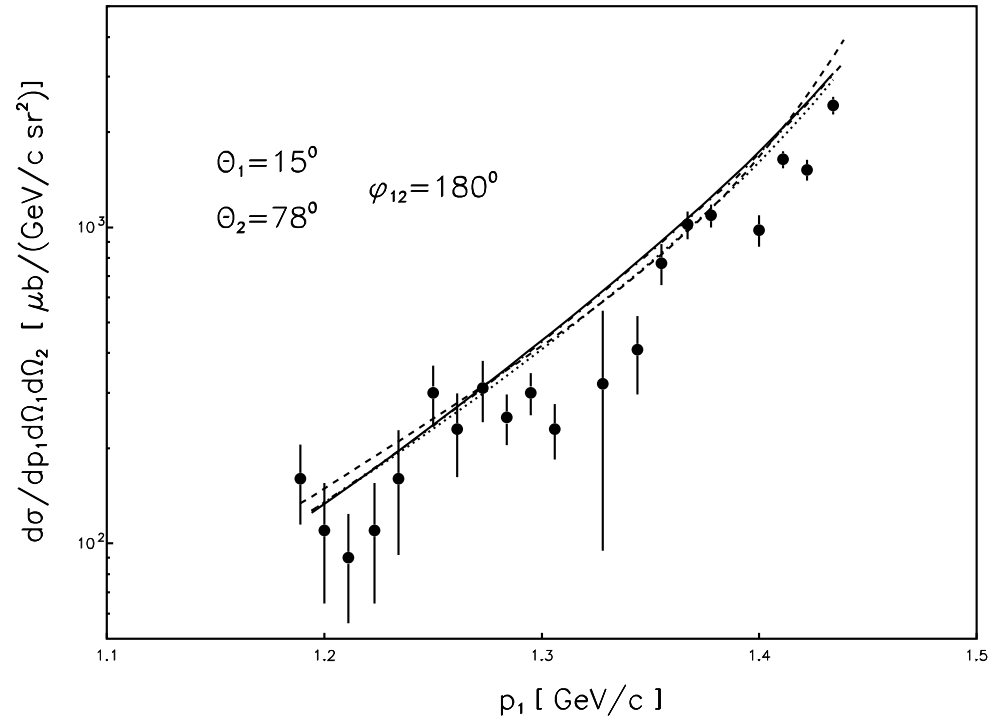


Fig.2

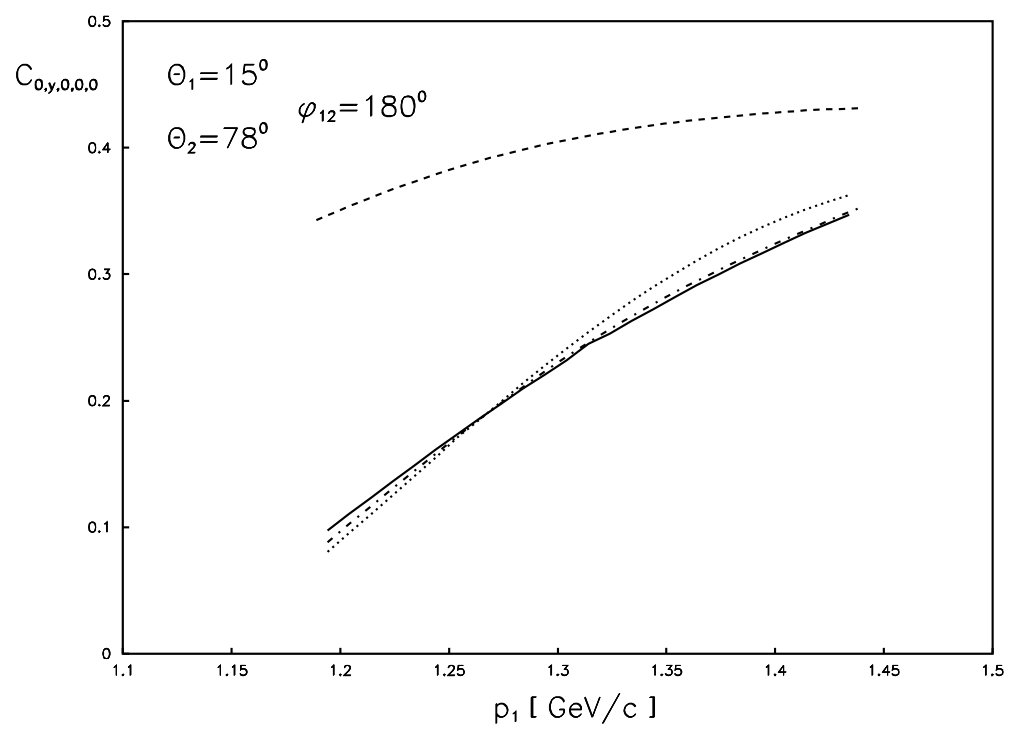


Fig.3

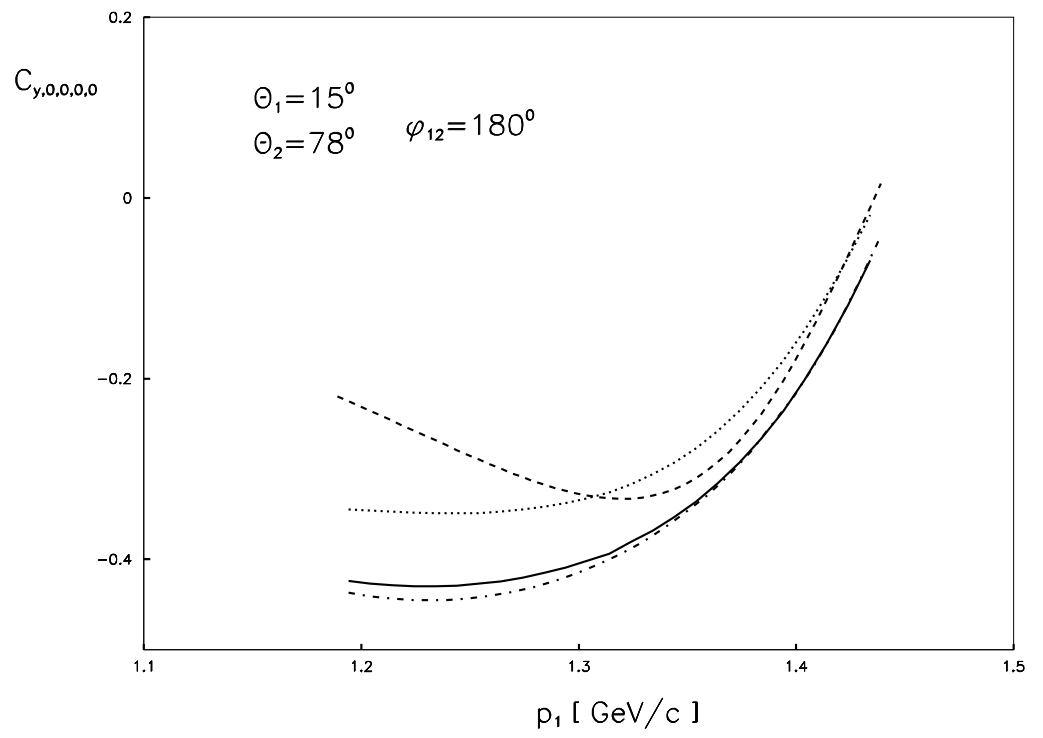


Fig.4

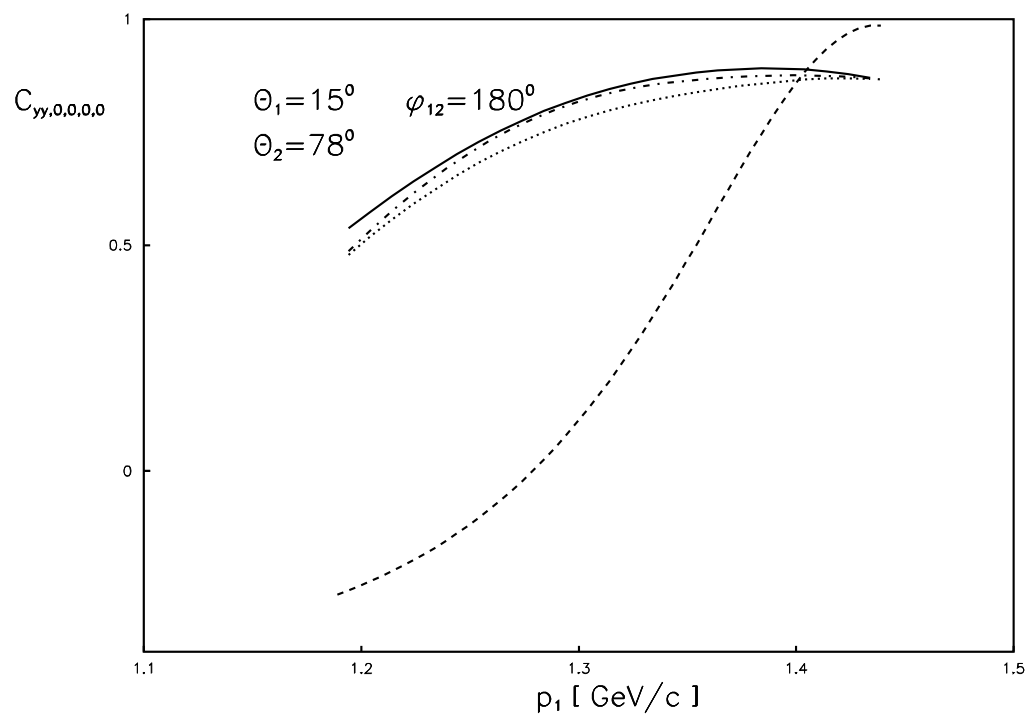


Fig.5

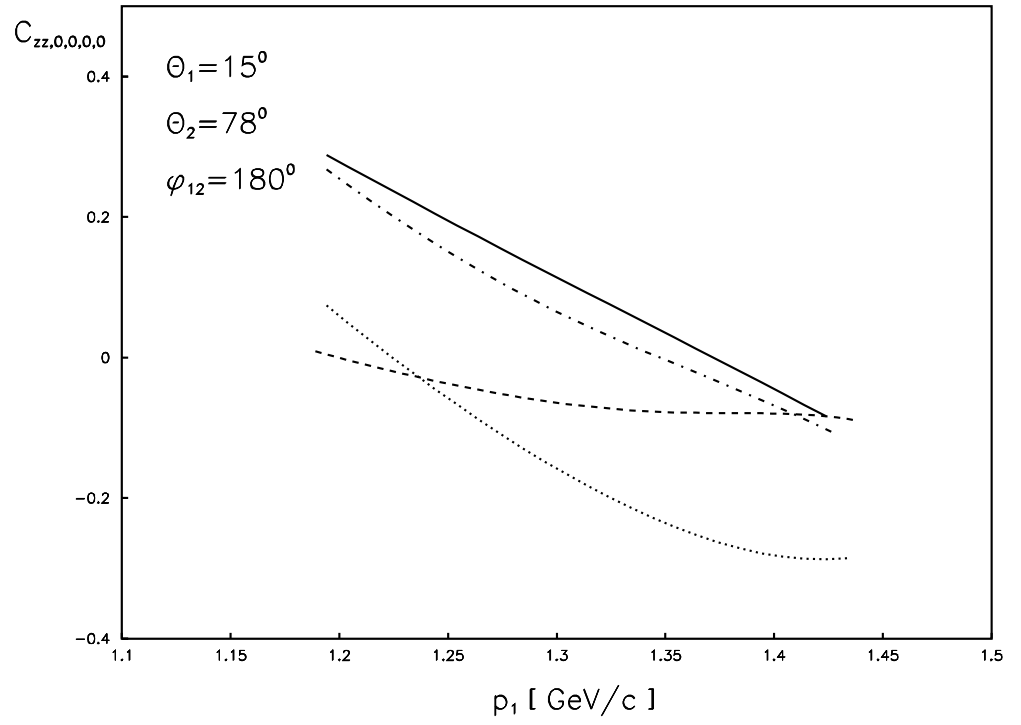


Fig.6

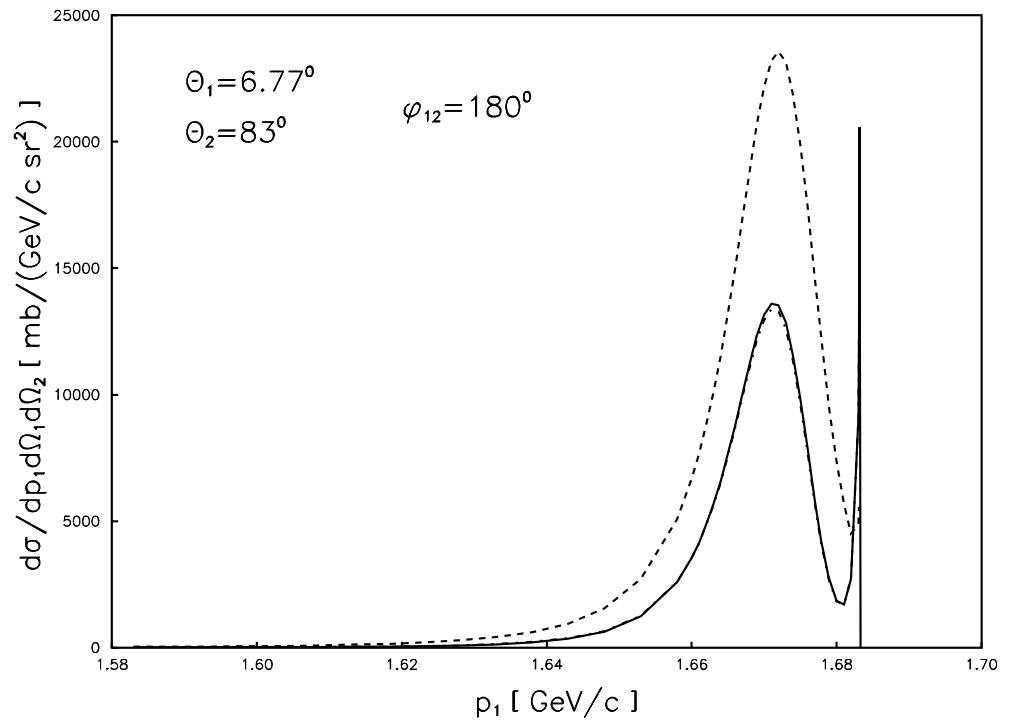


Fig.7

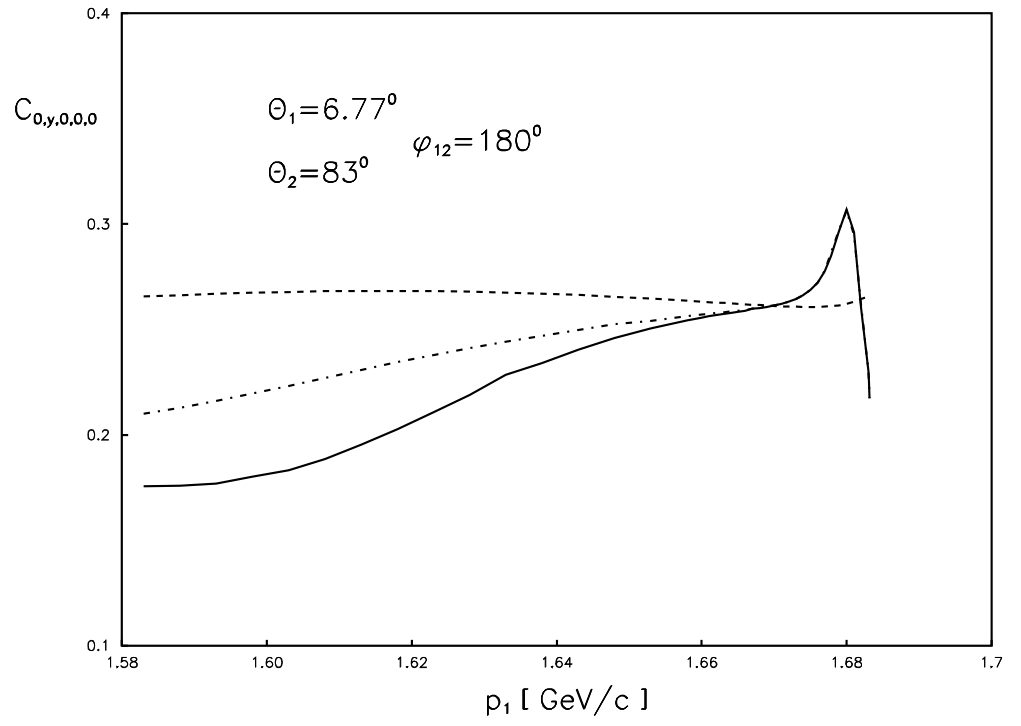


Fig.8



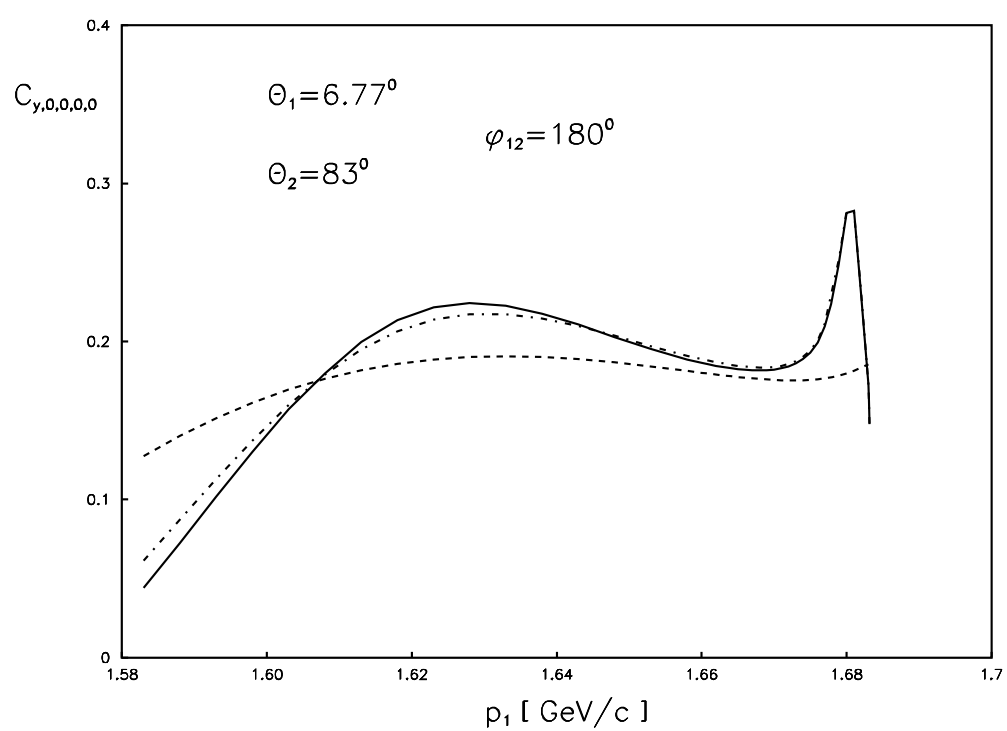


Fig.9

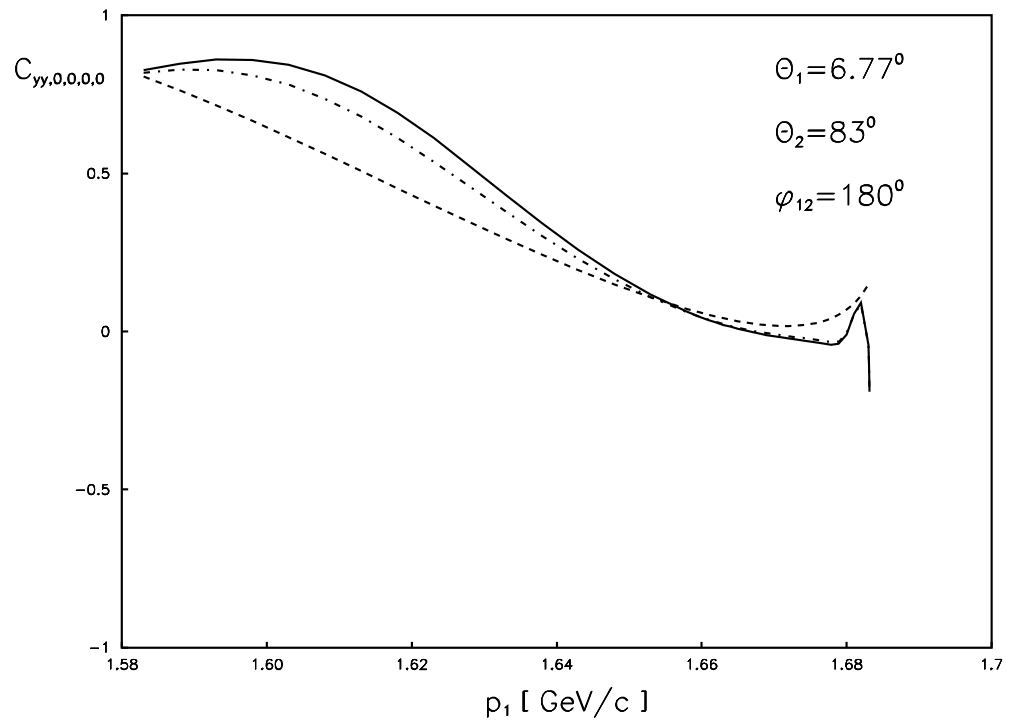


Fig.10

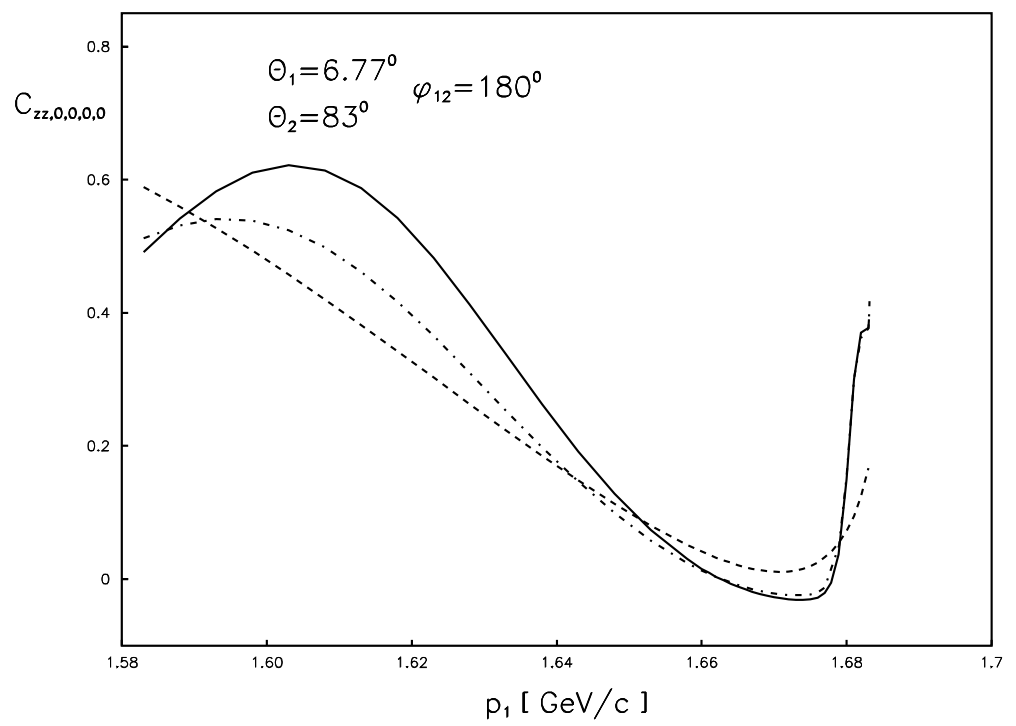


Fig.11